Heterogeneous ZnS-zinc carbonate hydroxide micro-belt for Cr(VI) reduction under simulated sunlight

Lei Bai*, Chun Kan, Xuejie Li, Yuanxin Zhou, Guoao Liang and Zirong Li*

College of Chemistry and Materials Engineering, Anhui Science and Technology University, Bengbu, 233010, China.

* Email: baileiwj2014@163.com; lizir@ahstu.edu.cn

Characterizations

X-ray diffraction (XRD) patterns were received using Shimadzu 6000 operating with Cu-K_α radiation with a scanning rate of $20^{o}\cdot min^{-1}$. X-ray Photoelectron Spectroscopy (XPS) was performed by a Thermo ESCALAB 250 instrument with a monochromatic Al Kα (hν = 1486.6 eV) X-ray source. Transmission electron microscopy (TEM) was performed using a JEOL JEM-2010 operated at 200 kV. High-resolution transmission electron microscopy (HRTEM) was performed on JEOL 2100, which was also operated at 200 kV. The UV–visible (UV-vis) diffuse reflectance spectra (DRS) of the samples were obtained on a UV–vis spectrophotometer (Shimadzu UV-3600, Lambda 850). Nitrogen adsorption/desorption isotherms were obtained at 77 K by using a Nova 2200 apparatus from Quantachrome Corporation, after having degassed the sample under vacuum at 393 K for 2 h. The specific area was calculated from the Brunauer–Emmett–Teller (BET) equation using P/P_0 values in the 0.05–0.25 range and the pore size distribution was obtained from the desorption branch using the Barrett–Joyner–Halenda (BJH) method. Time-resolved fluorescence (TRF) spectra of samples were detected by a fluorescence spectrofluorometer (Quantaurus-Tau, C11367, HAMAMATSU) under the 365 nm laser excitation at room temperature. UV–Vis absorption spectra of the solution were recorded on a Shimadzu UV-2600 spectrophotometer from 300 to 450 nm with a moderate scanning rate mode. All of electrochemical experiments were performed with a CHI-660E electrochemical workstation (CHI Instruments, USA). The photocurrent was carried out in a

conventional three-electrode cell using a Pt plate and an Ag/AgCl electrode as the counter electrode and reference electrode, respectively. The catalyst powder deposited on the fluoride tin oxide (FTO) substrate was used for the electrophotocatalytic analysis. The photocurrent transient response of the samples was performed in a 0.5 M Na_2SO_4 aqueous solution without bias versus Ag/AgCl electrode. The experiment of Mott-Schottky curves was performed in a three-electrode cell with a bulk film electrode (2 × 2 cm^2) as the working electrode, SCE as the reference electrode and a Pt strip as the counter electrode. Electrochemical impedance analysis was performed in a 0.5 M Na_2SO_4 solution using a frequency of 1000 Hz and an AC amplitude of 10 mV at each potential. The electron spin resonance (ESR) spectra which captured the $\cdot OH$ and $\cdot O_2^-$ generated by the samples under light irradiation with 5,5-dimethyl-1-pyrroline N-oxide (DMPO) were obtained on a Bruker model A300 Paramagnetic spectrometer.

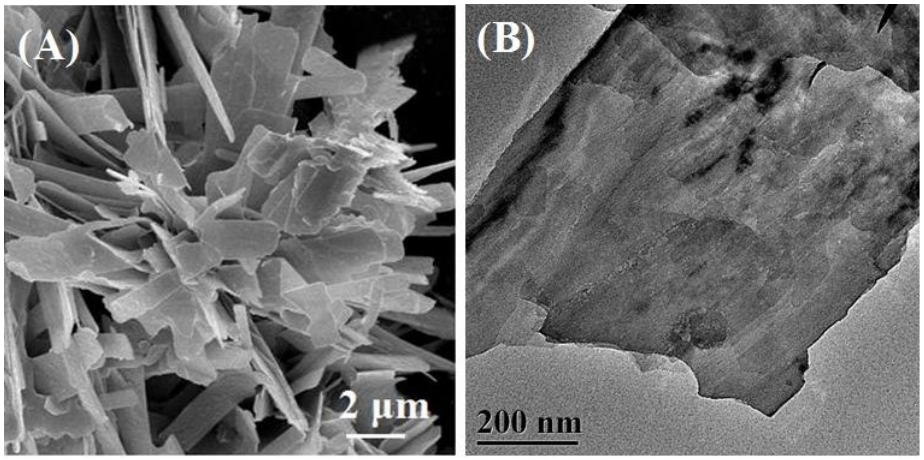

SFig.1 SEM (A) and TEM (B) image of ZCH.

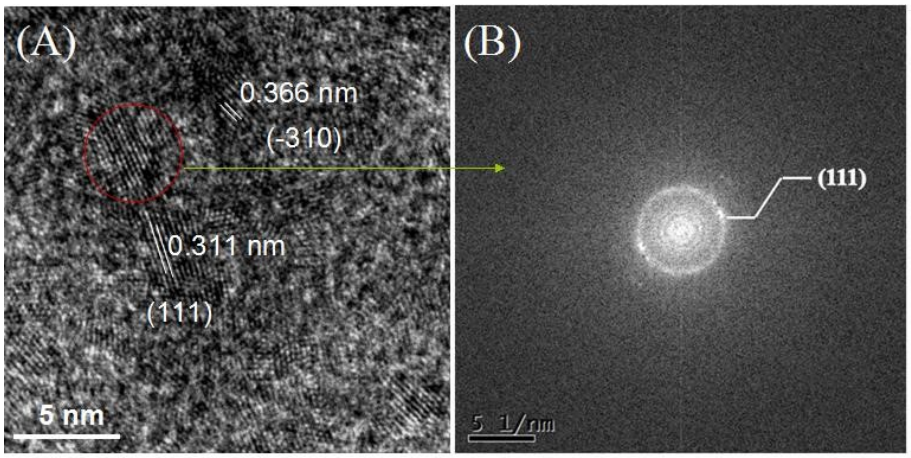

SFig.2 HRTEM image (A) and FFT pattern (B) of ZnS-ZCH.

New analysis was performed on the HRTEM result of ZnS-ZCH and as shwon in the above figure A, the lattice distance of 0.311 and 0. 366 nm were due to the (111) plane of ZnS (sphalerite) and (-310) plane of hydrozincite, respectively. Besides, the FFT pattern of the selected area confirmed the existence of ZnS (sphalerite), by calculated distance of (111) crystal plane. Thus, the information with the XRD pattern could prove the existence of heterogenesous structure.

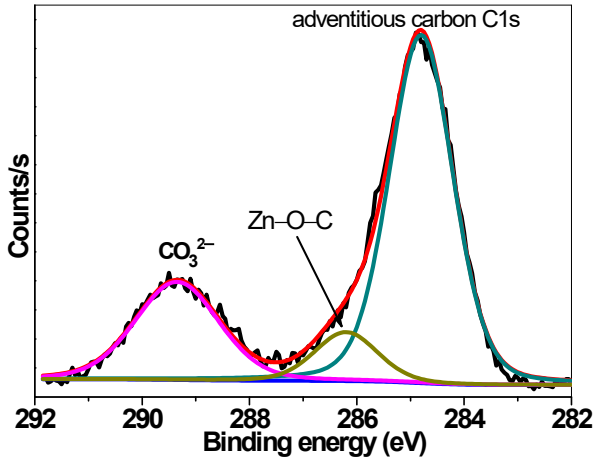

SFig.3 XPS spectrum of C1s of ZnS-ZCH.

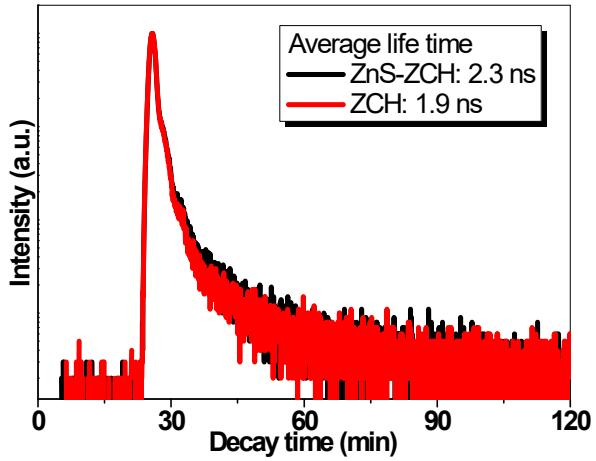

SFig.4 Time-resolved fluorescence spectra of ZCH and ZnS-ZCH.

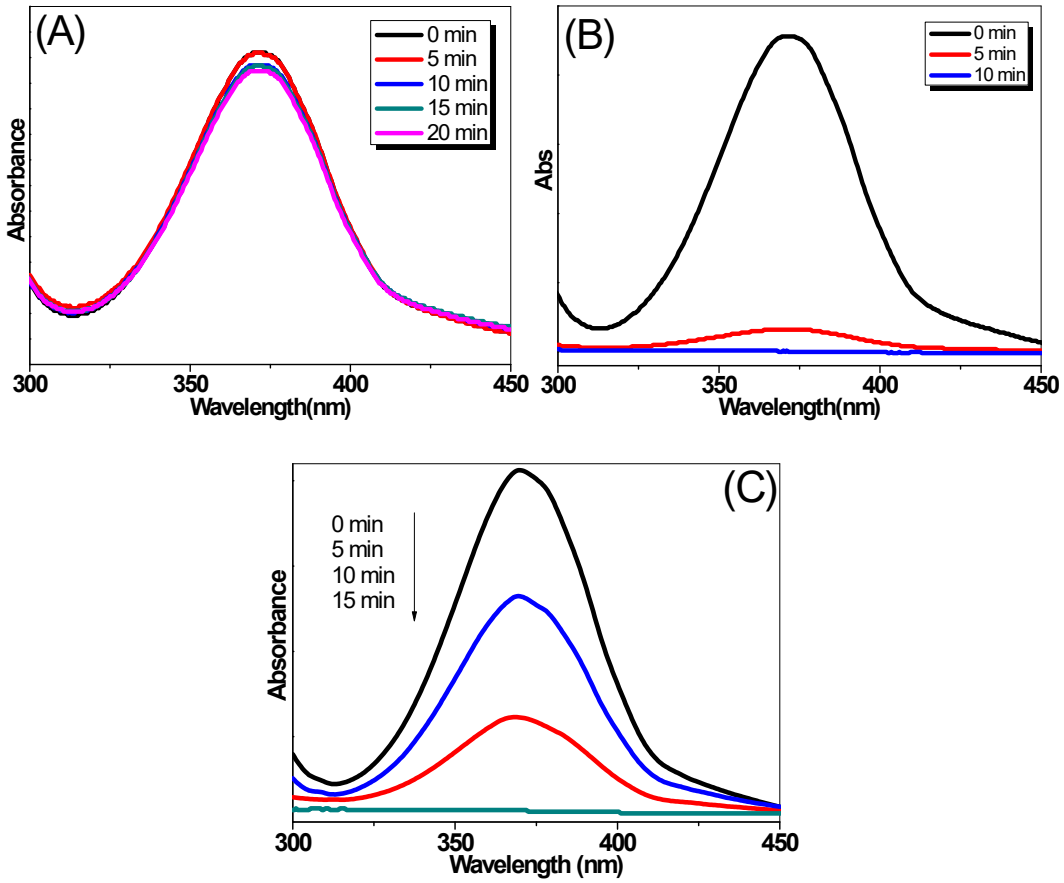

SFig.5 UV-vis spectra of Cr (VI) reduction in the presence of ZCH (A), ZnS-ZCH (B) and Degusa P25 (C).

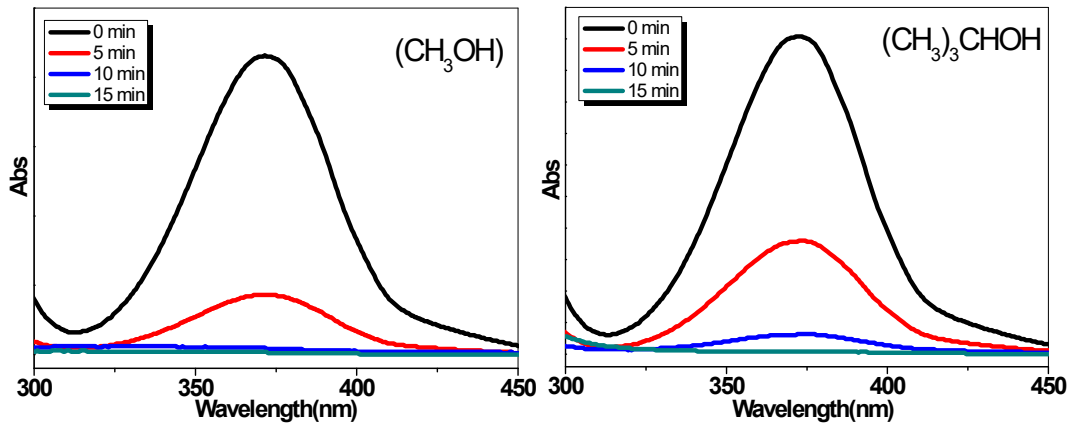

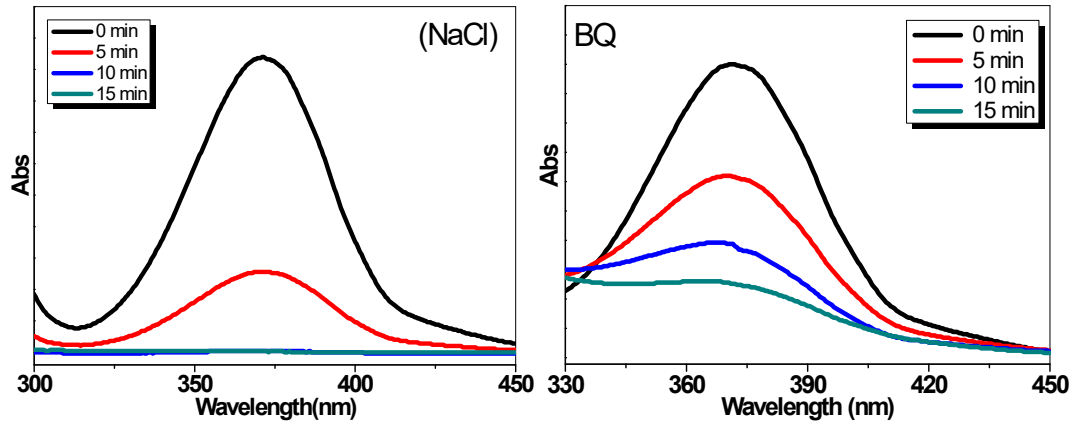

SFig.6 UV-vis spectra of Cr (VI) reduction in the presence of ZnS-ZCH with different additions.

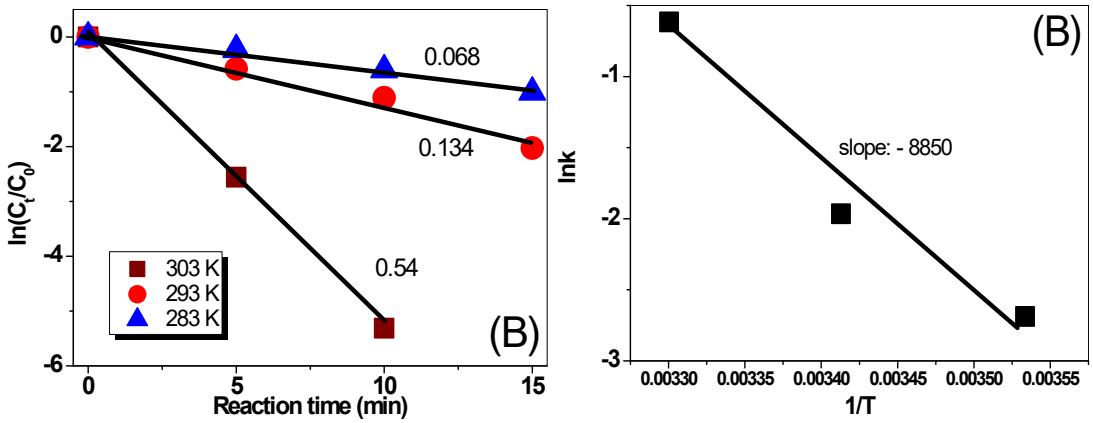

SFig.7 (A) The logarithm of the concentration vs. the reaction time at different temperatures and (B) ln *k* vs 1/T.

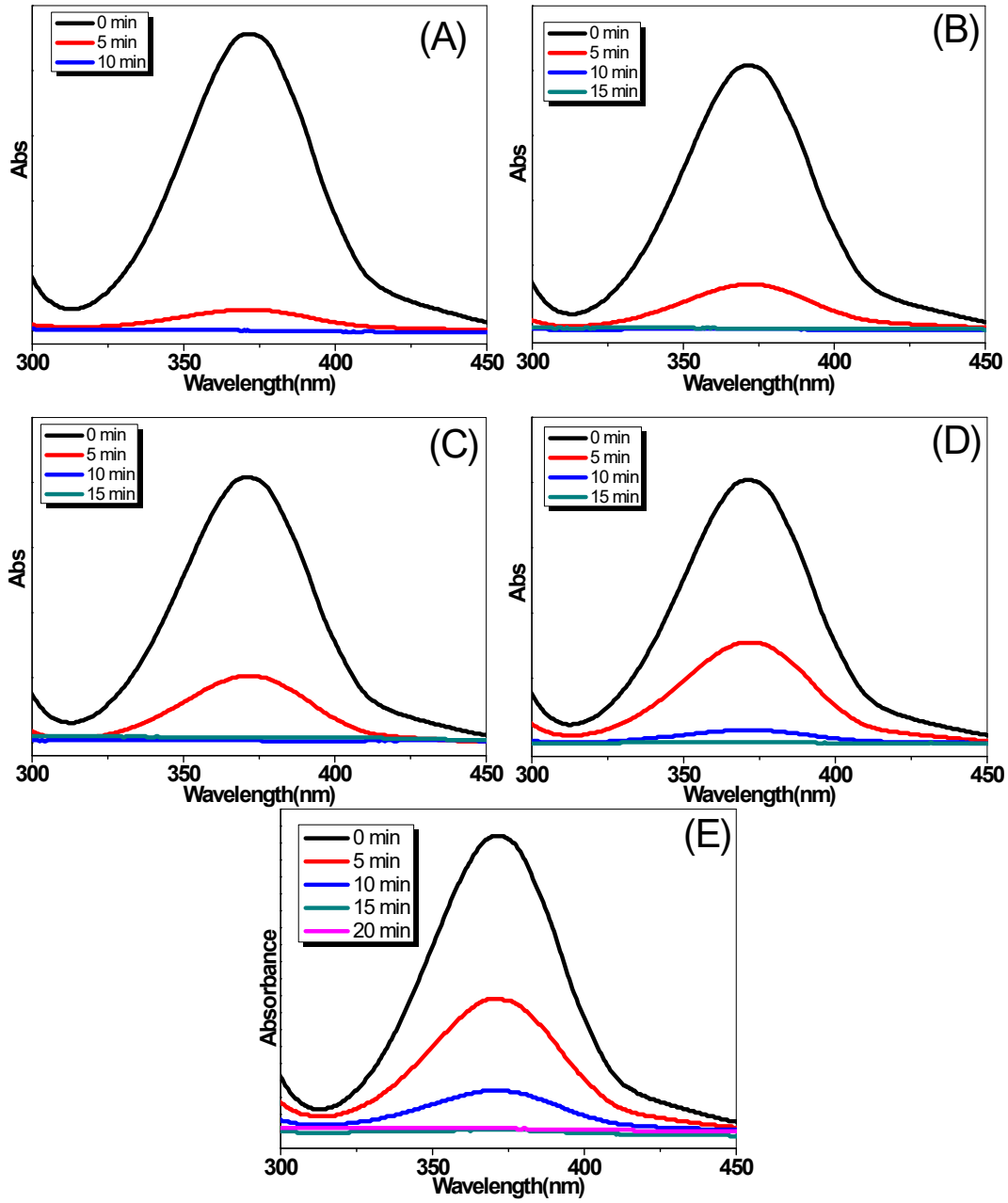

SFig.8 UV-vis spectra of Cr (VI) reduction in the presence of ZnS-ZCH from 1st to 5th run (A-E).

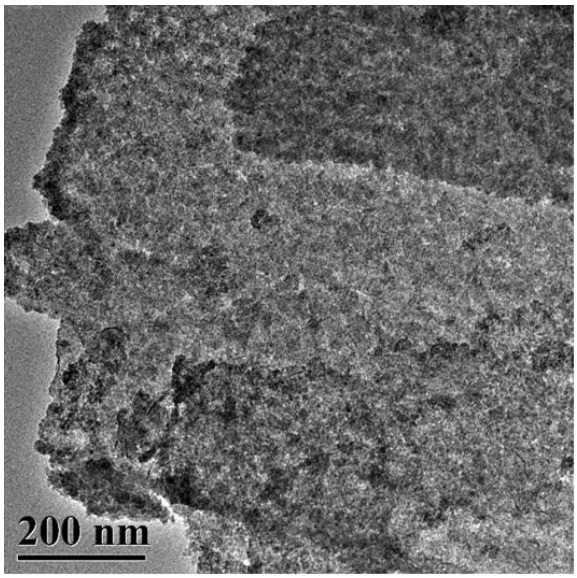

SFig.9 TEM image of ZnS-ZCH collected after reaction.

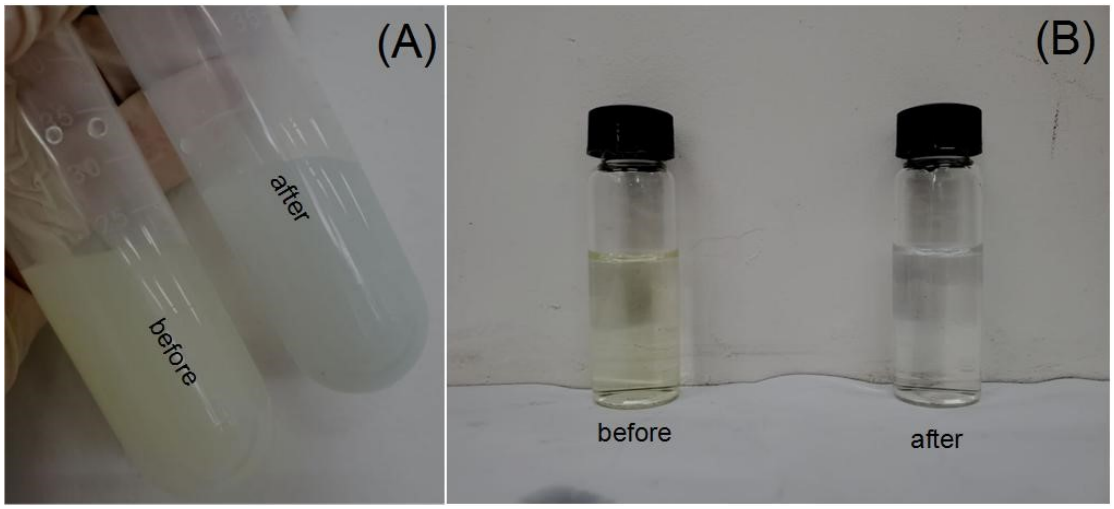

SFig.10 Pictures of reaction systems before and after light irradiation (A) and the water color before and after treatment (B).

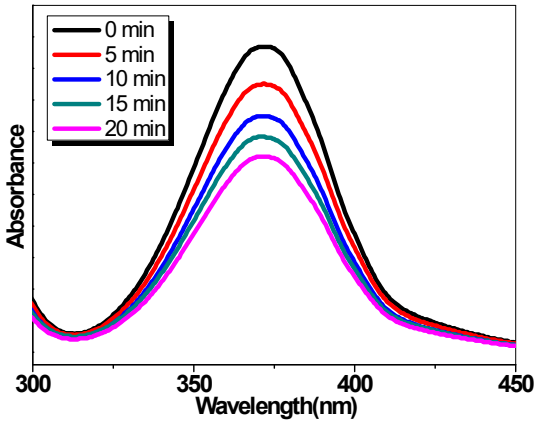

SFig.11 UV-vis spectra of Cr (VI) reduction in the presence of ZnS-ZCH under visible light (420~760 nm, 160 mW/cm^2).